

SUPPORTING INFORMATION

Ti₃C₂T_x (MXene) - wrapped V₂O₅/Fe₂O₃ composite for enhanced-performance supercapacitors

Yaqi Wang, Zhihu Pan, Xiaohong Ji*

School of Materials Science and Engineering, South China University of Technology,

Guangzhou 510641, China

*jxhong@scut.edu.cn

XPS survey spectrum of VFO/CC and core-level spectra of O 1s and C 1s

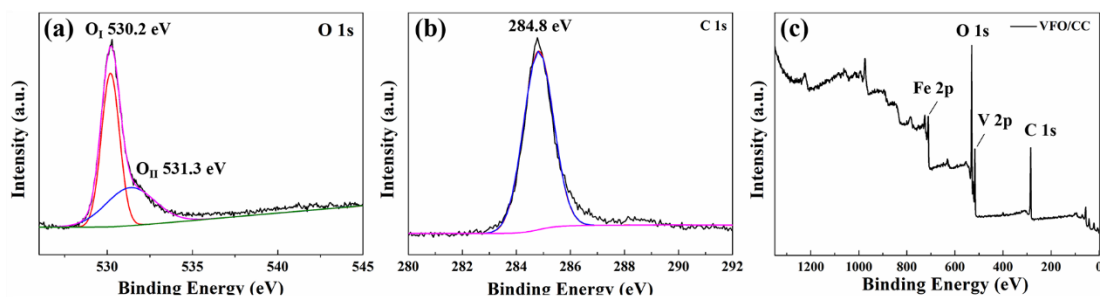


Fig. S1 (a) High-resolution XPS spectrum of O 1s. (b) High-resolution XPS spectrum of C 1s. (c)

XPS survey spectrum of the VFO/CC.

Electrochemical performance of VFO/CC-T electrodes

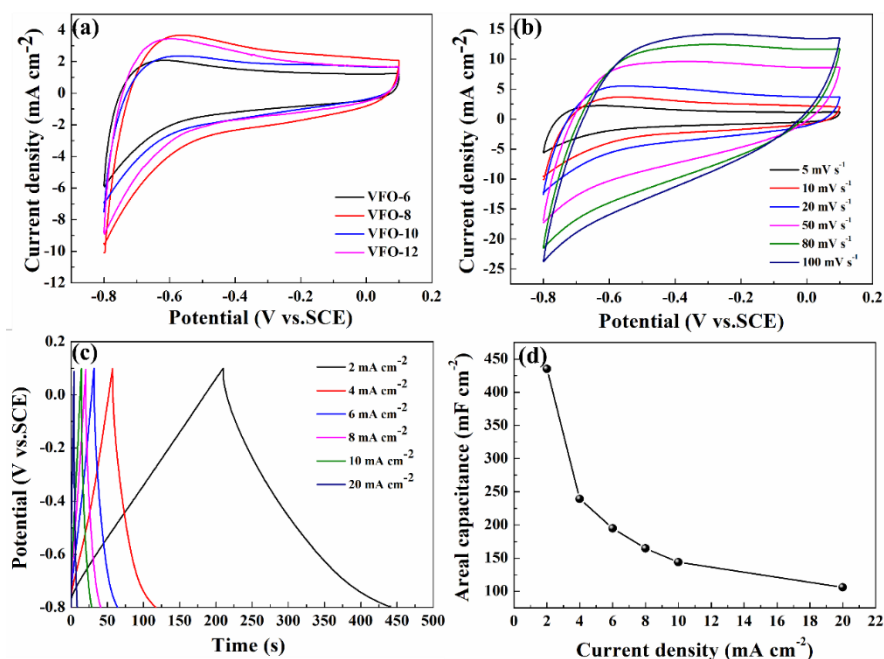


Fig. S2 (a) CV curves of VFO/CC-T at the scan rate of 10 mV s⁻¹. (b) CV curves of VFO/CC-8 at different scan rates. (c) GCD curves of VFO/CC-8 at different current densities. (d) The areal capacitance of VFO/CC-8 at different current densities.

The electrochemical performance of VFO@CC-T electrode was evaluated in the three-electrode configuration, 1M Na₂SO₄ was used as electrolyte solution, platinum plate as counter electrode and SCE as reference electrode, where T represents the hydrothermal time for the preparation of iron oxide nanorods. Fig. S2a shows the CV curves of VFO/CC-T at a scan rate of 10 mV s⁻¹. The VFO/CC-8 electrode has the largest integral area in the potential window of -0.8 ~ 0V, which indicates that the charge storage capacity of the sample is the highest when the hydrothermal time is 8h. Fig. S2b shows the CV curves of VFO/CC-8 at different sweep rates. There are weak redox peaks in the CV curves, which proves that the charge of the sample is stored by the pseudo capacitive energy storage mechanism. The sample VFO/CC-8 was tested by GCD at the current density of 2 mA cm⁻² to 20 mA cm⁻² (Fig. S2c). Fig. S2d shows the

variation trend of area capacitance of VFO/CC-8 calculated from GCD curve. The area capacitance is 435.2 mF cm^{-2} at 2 mA cm^{-2} . With the increase of current density, the capacitance of VFO/CC-8 decreases gradually. At 20 mA cm^{-2} , the area capacitance is 106 mF cm^{-2} (capacitance retention is 24.4%).

XPS survey spectrum of 2.0-Ti₃C₂T_x@VFO/CC

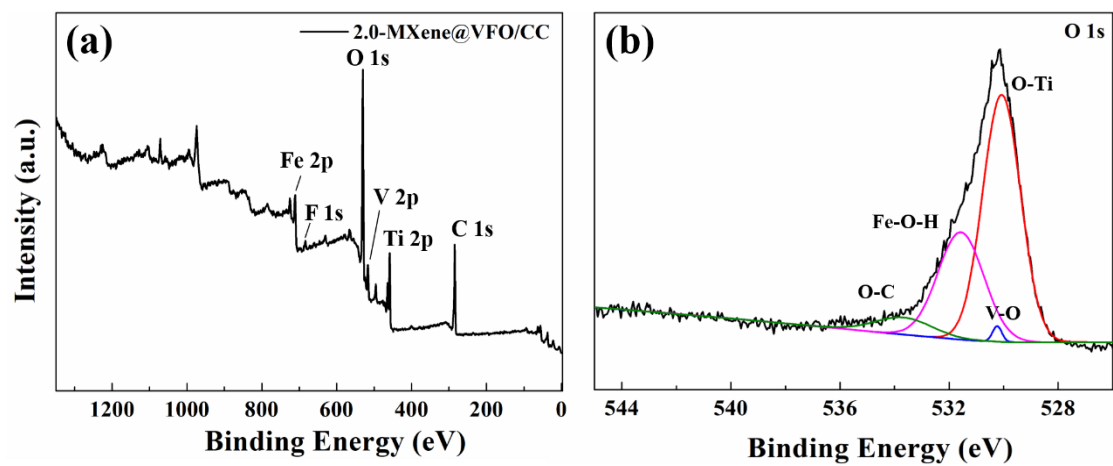


Fig. S3 (a) XPS survey spectrum of the 2.0-Ti₃C₂T_x@VFO/CC. (b) High-resolution XPS spectrum of O 1s.

Electrochemical performance of 3.0-Ti₃C₂T_x@VFO/CC-8 electrodes

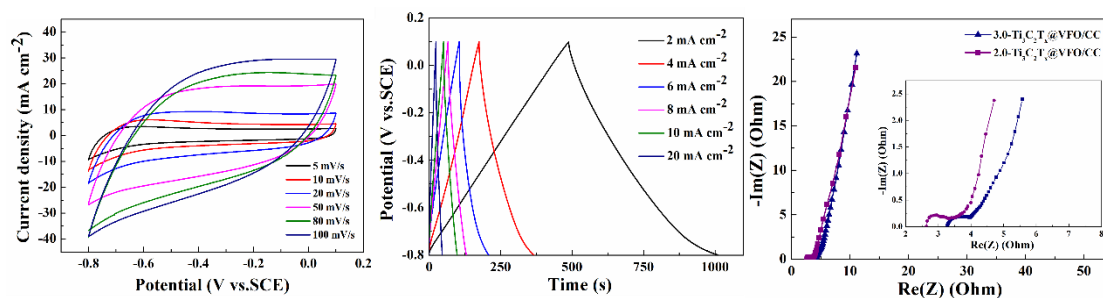


Fig. S4 (a) CV curves of 3.0-Ti₃C₂T_x@VFO/CC-8 at different scan rates. (b) GCD curves of 3.0-Ti₃C₂T_x@VFO/CC-8 at different current density. (c) Nyquist plots of 2.0-Ti₃C₂T_x@VFO/CC and 3.0-Ti₃C₂T_x@VFO/CC and the enlarged inset at high frequency.

The Nyquist test shows that the Ohmic impedance of 3.0-Ti₃C₂T_x@VFO/CC-8 is higher than 2.0-Ti₃C₂T_x@VFO/CC-8's, indicating that thicker Ti₃C₂T_x leads to larger impedance of the electrode.

Preparation of MnO₂ nanowires and its properties

The MnO₂ nanowire structures were synthesized on CC by the hydrothermal method at optimized condition. First, 0.1453 g manganese sulfate monohydrate and 0.3792 g potassium permanganate were dissolved in 40mL of DI water with stirring for 15 min. Then, this solution was transferred to a 100 mL Teflon-lined stainless-steel autoclave, and 2 pieces of carbon cloth was immersed in the autoclave and sealed and maintained at 140°C for 24h. The as obtained CC was removed from the autoclave and carefully rinsed with deionized water several times. Then, it was dried at 60°C for 6 h in air. The average mass loading of α -MnO₂ on the carbon cloth was about 7.6 mg cm⁻².

The structure of MnO₂ was studied by XRD. As shown in Fig. S5a, the diffraction peaks located at 12.74 °, 18.06 °, 28.75 °, 37.62 °, 42.03 °, 49.92 ° and 59.73 °, corresponding to (110), (200), (310), (301), (411) and (260) reflection planes of MnO₂ (JCPDS# 44-0141), respectively¹. Fig. S5b is the SEM image of MnO₂/CC. The surface of carbon cloth is fully covered by MnO₂ nanowires uniformly. In Fig. S5c, the CV curves of MnO₂/CC electrode at different scanning rates (5 ~ 100 mV s⁻¹) maintain a quasi-rectangular shape, and they tend to be more rectangular at lower scanning rates and elliptic at higher scanning rates. The change of its shape can be attributed to the rapid redox reaction on the surface caused by the ion adsorption/desorption in the electrolyte solution and the conversion of Mn valence state². As shown in Fig. S5d, the area capacitance of MnO₂/CC electrode at different current densities was calculated according to GCD curve. The area capacitance of MnO₂/CC was 765.47 mF cm⁻² at 10 mV/s. When the sweep speed reaches 100 mV/s, the area capacitance of MnO₂/CC was 254 mF cm⁻², and the capacitance retention was about 33.18%.

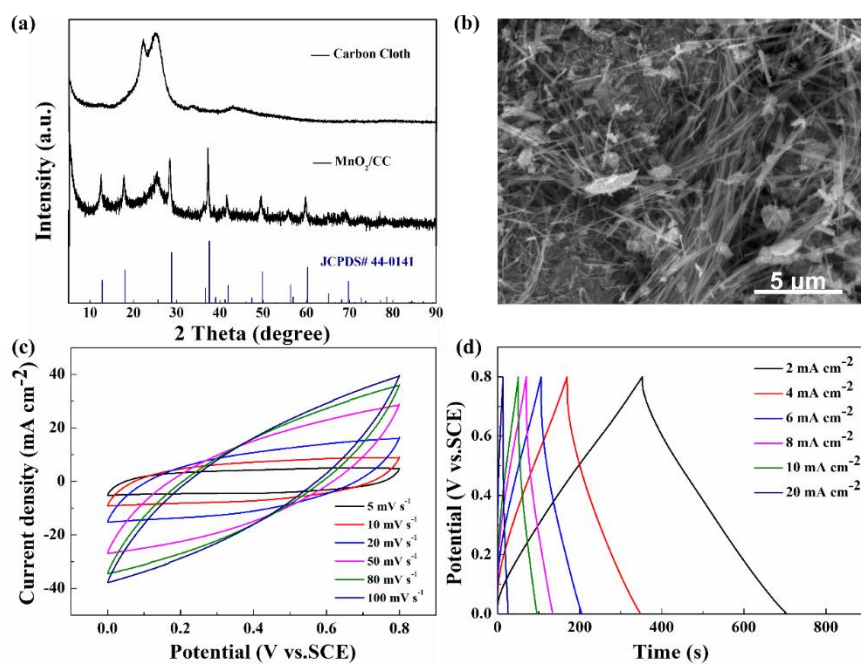


Fig. S5 (a) The XRD patterns of CC and MnO₂/CC. (b) The SEM image of MnO₂/CC. (c) CV curves of MnO₂/CC at different scan rates. (d) GCD curves of MnO₂/CC at different current density.

References:

- 1 Z.-H. Huang, Y. Song, D.-Y. Feng, Z. Sun, X. Sun and X.-X. Liu, High Mass Loading MnO₂ with Hierarchical Nanostructures for Supercapacitors, *ACS Nano*, 2018, **12**, 3557-3567.
- 2 P. Simon and Y. Gogotsi, Materials for electrochemical capacitors, *Nature Materials*, 2008, **7**, 845-854.